σ exchange in the nonmesonic decays of light hypernuclei and violation of the $\Delta I = 1/2$ rule

K. Sasaki,[1,*] M. Izaki,[2] and M. Oka[2]

[1]*Institute of Particle and Nuclear Studies, National Laboratory for High Energy Physics (KEK), 1-1, Oho, Tsukuba, 305-0801 Ibaraki, Japan*

[2]*Department of Physics, H27, Tokyo Institute of Technology, Meguro, Tokyo, 152-8551, Japan*

(Received 7 October 2004; published 17 March 2005)

Nonmesonic weak decays of *s*-shell hypernuclei are analyzed in microscopic models for the $\Lambda N \to NN$ weak interaction. A scalar-isoscalar meson σ is introduced, and its importance in accounting for the decay rates, n/p ratios, and proton asymmetry is demonstrated. Possible violation of the $\Delta I = 1/2$ rule in the nonmesonic weak decay of the Λ is discussed in a phenomenological analysis, and several useful constraints are presented. The microscopic calculation shows that the current experimental data indicate a large violation of the $\Delta I = 1/2$ rule, although no definite conclusion can be derived because of the large ambiguity of the decay rate of ${}^{4}_{\Lambda}\mathrm{H}$.

DOI: 10.1103/PhysRevC.71.035502 PACS number(s): 21.80.+a, 12.39.−x, 23.40.Bw

I. INTRODUCTION

Study of the nonmesonic weak decay (NMWD) of Λ hypernuclei is one of the major subjects of hypernuclear physics. A dominant contribution to NMWD is known to come from the $\Lambda N \to NN$ transition in nuclear medium, which is a new type of hadronic weak interaction. It is expected to provide us with valuable information on the weak interaction of quarks that may not be available in weak decays of hadrons. Recent progress in experimental research on the NMWD of various hypernuclear systems enables us to make quantitative comparison of theoretical predictions [1–18] and experimental data [19–26]. During such studies, several interesting discrepancies have been revealed.

One of the puzzling features is the so-called n/p problem, in which the ratio of the $\Lambda n \to nn$ decay rate Γ_n to the $\Lambda p \to pn$ decay rate Γ_p is underestimated in the simple one-pion-exchange (OPE) weak interaction. From a theoretical point of view, the essence of this puzzle is attributed to the strong tensor force brought by OPE. The n/p ratio is strongly suppressed (to about 0.1) by the enhancement of Γ_p due to the tensor force of OPE. Recent experimental data, however, established that the n/p ratio is around 1/2 for ${}^{5}_{\Lambda}\mathrm{He}$ and ${}^{12}_{\Lambda}\mathrm{C}$. In previous studies [8,14,15,18], we found that the total decay rates and n/p ratios are both sensitive to short-range components of the baryonic weak interaction, which are represented by the one-kaon exchange (OKE), and to the direct-quark (DQ) transition. We showed in the OPE+OKE+DQ model that Γ_n is enhanced by the short-range contributions and thus the model can reproduce the observed n/p ratio both in nuclear matter and in light hypernuclei. At the same time, we found that the total decay rates of light hypernuclei tend to be overestimated.

Another quantity that shows discrepancy between experiment and theory is the asymmetry of emitted protons from polarized hypernuclei. Recent theoretical predictions [13,15,18,27] yield large negative values of the asymmetry parameter α, while new experimental data suggest a smaller positive asymmetry for ${}^{5}_{\Lambda}\mathrm{He}$ decay [26]. The asymmetry comes from interference between the parity-conserving (PC) and the parity-violating (PV) parts of the decay amplitudes, and thus it is sensitive to the detail decomposition of the decay amplitudes. In other words, asymmetry has more discriminative power to determine goodness of the models than the decay rates have.

Besides the calculations with microscopic models, an analysis employing an effective field theory (EFT) was carried out recently [28,29]. In that analysis, the short-range parts of the interactions are represented by four-point baryonic operators. By fitting strength parameters to current experimental data, including the proton asymmetry, it revealed that the largest term comes from the isospin- and spin-independent central operator. Thus the EFT approach suggests that in order to reproduce the proton asymmetry data, the microscopic models should be supplemented by central interactions.

Following the hint given by this observation, we consider scalar-meson exchange in the weak $\Lambda N \to NN$ transition. The scalar σ meson with $I = 0$ has been introduced in the context of chiral symmetry of QCD. When the symmetry is spontaneously broken due to nonzero quark condensate, the pion π appears as a (pseudo) Nambu-Goldstone boson, while its chiral partner is a scalar-isoscalar σ for the $N_f = 2$ chiral symmetry. Although the picture of chiral symmetry breaking of QCD has been established for some time, existence of σ as a real meson was not confirmed until recently. It appears as a broad resonance in the π-π scattering phase shift, and its mass happens to be around 600 MeV [30]. It has been long known that strong *NN* potential requires the σ exchange in order to obtain enough attraction in both the spin singlet and triplet channels. As the σ mass is of the same range as the kaon, it is natural to expect its significant role in the weak baryonic interaction as well. Thus, we consider the one-sigma exchange (OSE) in $\Lambda N \to NN$ transition.

Our model, which we call DQ+, now consists of OPE, OKE, OSE, and DQ. We will show in this paper that the model contains the necessary features to reproduce all the experimental data on NMWD of light hypernuclei and that

*Electronic address: kenjis@post.kek.jp.

indeed the proton asymmetry puzzle can be solved by the contribution of OSE.

Another interesting property of the strangeness-changing weak interactions of hadrons is its isospin property. It is well known that the decays of kaon and hyperons satisfy the so-called $\Delta I = 1/2$ rule, which indicates the dominance of the $I = 1/2$ transition operator to the $I = 3/2$ operator. In the standard theory of the weak interaction of quarks, the transition $s + \bar{u} \to W^- \to d + \bar{u}$ allows both $\Delta I = 1/2$ and 3/2. Yet, in the hadron decays, the $\Delta I = 3/2$ transition is much weaker than the $\Delta I = 1/2$. The ratio of the amplitude is typically 20 in the decays of K and hyperons. The origin of this empirical "rule" is not completely understood. In $K \to \pi\pi$ decays, $\Delta I = 1/2$ dominance may be explained by contribution of the scalar-isoscalar meson σ in the s channel [31]. The enhancement is caused by the closeness of the masses of K and σ. Suppression of the $\Delta I = 3/2$ transition in the baryon weak decays may be explained by the color structure of the quark model wave function of the baryon [Miura-Minamikawa and Pati-Woo (MMPW) theorem] [32,33]. These mechanisms are rather specific to the particular decays and are not generalized to the nonmesonic weak decays, $YN \to NN$.

It is therefore important and interesting to test whether the $\Delta I = 1/2$ rule is also effective in NMWD of hypernuclei. This is the second purpose of this paper. We note that the meson exchange processes are all dominated by the $\Delta I = 1/2$ amplitudes. First OPE is assumed to be purely $\Delta I = 1/2$ because the $\pi\Lambda N$ weak vertex causes free Λ decay. From the $\Delta I = 1/2$ dominance of the $\Lambda \to N\pi$ decays, we expect that the vertex is (almost) purely $\Delta I = 1/2$. OKE is also supposed to have only $\Delta I = 1/2$, because the KNN weak coupling is derived from the $\pi\Lambda N$ coupling using the SU(3) relation. It is obvious that OSE, or the weak $\sigma\Lambda N$ coupling, is also purely $\Delta I = 1/2$, because the isospin of σ is zero.

In contrast, the DQ process may contain $\Delta I = 3/2$ transitions. We employ the effective weak Lagrangian derived from the standard theory with one-loop QCD corrections [34]. The perturbative QCD corrections, which are valid only at the momentum scale of M_W, are "improved" by using the QCD renormalization group equation. The resulting effective Lagrangian is given in terms of four-quark local operators such as $(\bar{d}_L u_L)(\bar{u}_L s_L)$. A part of the $\Delta I = 1/2$ enhancement (and $\Delta I = 3/2$ suppression) is included in the course of the down-scaling according to the renormalization group equation, but certain $\Delta I = 3/2$ strength still remains [35,36]. The DQ transition potential thus contains a $\Delta I = 3/2$ part.

In the previous study, we predicted significant violation of the $\Delta I = 1/2$ rule in the $J = 0$ transition amplitudes in particular. In this paper, we consider how the $\Delta I = 3/2$ transition affects the transition rates of light hypernuclei and check the validity of the $\Delta I = 1/2$ rule within the available experimental data.

This paper is organized as follows. In Sec. II, we summarize the formulation of the weak transition calculations. In Sec. III, several general relations based on simple parametrization of the decay rates of the s-shell hypernuclei are given, and the validity of the $\Delta I = 1/2$ rule is considered. In Sec. IV, we introduce the σ exchange and complete our DQ+ model. The weak coupling parameters for the σ meson are determined so as to reproduce data from the s-shell hypernuclei. We give the full results including the proton asymmetry parameter and point out the important roles of the σ meson exchanges. Conclusions are given in Sec. V.

TABLE I. Possible $^{2S+1}L_J$ combinations and amplitudes for nonmesonic weak transitions of the s-shell hypernuclei.

State		Parity	isospin	Amplitude	
Initial	final			$I_z^f = 0$	$I_z^f = -1$
$^1S_0$	$^1S_0$	PC	$I^f = 1$	a_p	a_n
	$^3P_0$	PV	$I^f = 1$	b_p	b_n
$^3S_1$	$^3S_1$	PC	$I^f = 0$	c_p	—
	$^3D_1$	PC	$I^f = 0$	d_p	—
	$^1P_1$	PV	$I^f = 0$	e_p	—
	$^3P_1$	PV	$I^f = 1$	f_p	f_n

II. DECAY RATES OF LIGHT HYPERNUCLEI

Observables of the weak decay of s-shell hypernuclei give us a chance to discuss the properties of the $\Lambda N \to NN$ interaction, the Γ_n/Γ_p ratio, and the $\Delta I = 1/2$ dominance. Block and Dalitz [37] performed an analysis based on the lifetime data of light hypernuclei, which were updated by other authors [38,39].

For s-shell hypernuclei, the initial ΛN system can be assumed to be in the relative s-wave state, and we consider the $\Lambda N \to NN$ transition with the six $^{2S+1}L_J$ combinations listed in Table I.

Using amplitudes $a_p \sim f_n$, we can express the total decay rates of light hypernuclei in the short-handed notation

$$\Gamma_{NM}\left({}^5_\Lambda\mathrm{He}\right) = \left|a_p^5\right|^2 + \left|b_p^5\right|^2 + 3\left(\left|c_p^5\right|^2 + \left|d_p^5\right|^2 + \left|e_p^5\right|^2 + \left|f_p^5\right|^2\right) + \left|a_n^5\right|^2 + \left|b_n^5\right|^2 + 3\left|f_p^5\right|^2, \quad (1)$$

$$\Gamma_{NM}\left({}^4_\Lambda\mathrm{He}\right) = \left|a_p^4\right|^2 + \left|b_p^4\right|^2 + 3\left(\left|c_p^4\right|^2 + \left|d_p^4\right|^2 + \left|e_p^4\right|^2 + \left|f_p^4\right|^2\right) + 2\left(\left|a_n^4\right|^2 + \left|b_n^4\right|^2\right), \quad (2)$$

$$\Gamma_{NM}\left({}^4_\Lambda\mathrm{H}\right) = 2\left(\left|a_p^4\right|^2 + \left|b_p^4\right|^2\right) + \left|a_n^4\right|^2 + \left|b_n^4\right|^2 + 3\left|f_p^4\right|^2, \quad (3)$$

where the superscript indicates the mass number of the hypernucleus. Similarly, the n/p ratios of light hypernuclei are written as

$$\frac{\Gamma_n}{\Gamma_p}\left({}^5_\Lambda\mathrm{He}\right) = \frac{\left|a_n^5\right|^2 + \left|b_n^5\right|^2 + 3\left|f_p^5\right|^2}{\left|a_p^5\right|^2 + \left|b_p^5\right|^2 + 3\left(\left|c_p^5\right|^2 + \left|d_p^5\right|^2 + \left|e_p^5\right|^2 + \left|f_p^5\right|^2\right)}, \quad (4)$$

$$\frac{\Gamma_n}{\Gamma_p}\left({}^4_\Lambda\mathrm{He}\right) = \frac{2\left(\left|a_n^4\right|^2+\left|b_n^4\right|^2\right)}{\left|a_p^4\right|^2+\left|b_p^4\right|^2+3\left(\left|c_p^4\right|^2+\left|d_p^4\right|^2+\left|e_p^4\right|^2+\left|f_p^4\right|^2\right)}, \tag{5}$$

$$\frac{\Gamma_n}{\Gamma_p}\left({}^4_\Lambda\mathrm{H}\right) = \frac{\left|a_n^4\right|^2+\left|b_n^4\right|^2+3\left|f_n^4\right|^2}{2\left(\left|a_p^4\right|^2+\left|b_p^4\right|^2\right)}. \tag{6}$$

The asymmetry parameter [40] is obtained by

$$\alpha = \frac{2\left(-\sqrt{3}\left[a_p^5 e_p^5\right]-\left[b_p^5 c_p^5\right]+\sqrt{2}\left[b_p^5 d_p^5\right]+\sqrt{6}\left[c_p^5 f_p^5\right]+\sqrt{3}\left[d_p^5 f_p^5\right]\right)}{\left|a_p^5\right|^2+\left|b_p^5\right|^2+3\left(\left|c_p^5\right|^2+\left|d_p^5\right|^2+\left|e_p^5\right|^2+\left|f_p^5\right|^2\right)}, \tag{7}$$

where we define $[a_p e_p] \equiv \mathrm{Re}(a_p^* e_p)$, etc. Note that interference terms appear between the $J=0$ and $J=1$ amplitudes, such as $[a_p e_p]$ and $[b_p c_p]$, in Eq. (7).

The $\Delta I = 1/2$ rule for the $\Lambda N \to NN$ transition leads to the isospin relations

$$a_n = \sqrt{2}a_p, \quad b_n = \sqrt{2}b_p, \quad \text{and} \quad f_n = \sqrt{2}f_p \tag{8}$$

for the decay amplitudes listed in Table I. This rule also makes

$$\kappa \equiv \frac{\Gamma_n\left({}^4_\Lambda\mathrm{He}\right)}{\Gamma_p\left({}^4_\Lambda\mathrm{H}\right)} = \frac{\left|a_n^4\right|^2+\left|b_n^4\right|^2}{\left|a_p^4\right|^2+\left|b_p^4\right|^2} \tag{9}$$

to be equal to 2. Therefore the κ is important to check the validity of the $\Delta I = 1/2$ rule for the $\Lambda N \to NN$ transition from both the theoretical and experimental points of view.

In the present analysis, we do not take into account virtual Σ mixing in hypernuclei. Importance of the Σ mixing in ${}^4_\Lambda$He and ${}^4_\Lambda$H was pointed out elsewhere [18,41–45]. Even if the microscopic interactions preserve the $\Delta I = 1/2$ rule, the Λ-Σ mixing may result in deviation from the $\Delta I = 1/2$ relation: $\kappa = 2$. We also neglect decay amplitudes that are induced by two nucleons, i.e., $\Lambda NN \to NNN$ decays. This is another process that may modify the above relations. Thus, strictly speaking, we need to subtract those extra contributions before applying the above relations to the experimental data.

The $\Lambda N \to NN$ transition rate is given by

$$\Gamma_N = \int \frac{d^3p_1'}{(2\pi)^3}\int \frac{d^3p_2'}{(2\pi)^3}\frac{1}{2J_H+1}\sum_{i,f}(2\pi)\delta(E_f-E_i)|M_{fi}|^2, \tag{10}$$

where M_{fi} is the $\Lambda N \to NN$ transition amplitude, J_H is the total spin of initial hypernucleus, and p'_1 and p'_2 are momenta of emitted particles, i.e., hyperon and nucleon. The summation indicates a sum over all quantum numbers of the initial and final particle systems.

After the decomposition of angular momentum, the explicit form of $|M_{fi}|^2$ is

$$|M_{fi}|^2 = (4\pi)^4\left|\int\int\int \Psi_f^{L'S'J}(R,r')V_{SS'J}^{LL'}(r,r') \times \Psi_i^{LSJ}(R,r)r^2dr r'^2dr'R^2dR\right|^2, \tag{11}$$

where $V_{SS'J}^{LL'}(r,r')$ is the (nonlocal) transition potential and $\Psi^{LSJ}(R,r)$ is the wave function of the ΛN or NN two-body system in the configuration space. The indices L, S, and J indicate the orbital angular momentum, spin, and total spin for the two-body system, respectively.

We take the wave function of the Λ-N two-body system in the form

$$\phi_Y(\vec{r}_Y)\phi_N(\vec{r}_N)\left[\left(1-e^{-r^2/a^2}\right)^n - br^2e^{-r^2/c^2}\right], \tag{12}$$

where ϕ_i stands for a single-particle wave function inside the nucleus, and $r = |\vec{r}_Y - \vec{r}_N|$. For ϕ_N, we assume the harmonic oscillator shell model, and the size parameter is chosen so as to reproduce the size of the nucleus without Λ. The ϕ_Λ is described by the solution of the Schrödinger equation with a Λ-core potential [14]. The parameters for the short-range correlation are $a = 0.5$ fm, $b = 0.25$ fm^{-2}, $c = 1.28$ fm, and $n = 2$, which reproduce the realistic Λ-N correlation [13].

The wave function of the final two nucleons emitted in the two-body weak process is assumed to be the plane wave with the short-range correlation

$$e^{i\vec{K}\cdot\vec{R}'}e^{i\vec{k}\cdot\vec{r}'}[1-j_0(q_c r')], \tag{13}$$

where $\vec{r}' = \vec{r}_{N_2} - \vec{r}_{N_1}$, $\vec{R}' = (\vec{r}_{N_2} + \vec{r}_{N_1})/2$, and $q_c = 3.93$ fm^{-1}. This approximation may be justified for light nuclei as the momenta of the emitted nucleons are relatively high ($\sim$400 MeV/c).

The general form of the one-pion-exchange (OPE) potential for the $\Lambda N \to NN$ transition can be written as

$$V_{\Lambda N\to NN}(\vec{q}) = g_s[\bar{u}_N\gamma_5 u_N]\frac{1}{\vec{q}^2+\tilde{m}_i^2}\left(\frac{\Lambda_i^2-\tilde{m}_i^2}{\Lambda_i^2+\vec{q}^2}\right)^2 \times g_w[\bar{u}_N(A+B\gamma_5)u_\Lambda], \tag{14}$$

where the coupling constants g_s, g_w, A, and B, shown in Table II, are chosen properly for each transition. It is easy to confirm that the weak coupling constants satisfy the $\Delta I = 1/2$ conditions, namely, $A_{\pi^-\Lambda p} = -\sqrt{2}A_{\pi^0\Lambda n}$ and $B_{\pi^-\Lambda p} = -\sqrt{2}B_{\pi^0\Lambda n}$. A monopole form factor with cutoff parameter $\Lambda_\pi = 800$ MeV is employed for each vertex. As the energy transfer is significantly large, we introduce the effective meson mass

$$\tilde{m} = \sqrt{m^2-(q^0)^2}, \qquad q^0 = 88.5\,\mathrm{MeV}. \tag{15}$$

TABLE II. The strong and weak coupling constants in the present model. The strong couplings are taken from the Nijmegen soft-core potential (NSC97) [46]. The weak couplings are given in units of $g_w \equiv G_F m_\pi^2 = 2.21 \times 10^{-7}$. The weak coupling constants for σ meson are the values used in Sec. IV.

Meson (mass)	Strong c.c.	Weak c.c.	
		PC	PV
π (138 MeV)	$g_{NN\pi} = 13.16$	$B_{\pi^0\Lambda n} = 7.15$	$A_{\pi^0\Lambda n} = -1.05$
		$B_{\pi^-\Lambda p} = -10.11$	$A_{\pi^-\Lambda p} = 1.48$
K (495 MeV)	$g_{\Lambda NK} = -17.65$	$B_{K^0nn} = -16.19$	$A_{K^0nn} = 2.83$
		$B_{K^0pp} = 6.65$	$A_{K^0pp} = 2.09$
		$B_{K^+pn} = -22.84$	$A_{K^+pn} = 0.76$
σ (550 MeV)	$g_{NN\sigma} = 13.16$	$A_\sigma^{ME} = 3.8$	$B_\sigma^{ME} = 1.2$
		$A_\sigma^{DQ+} = 3.9$	$B_\sigma^{DQ+} = 6.6$

The one-kaon-exchange (OKE) potential can be constructed similarly. Both the strong and weak coupling constants are evaluated using the flavor SU(3) symmetry; they are also listed in Table II. The cutoff parameter $\Lambda_K = 1300$ MeV is used for the form factor. The $\Delta I = 1/2$ rule for the weak KNN vertex requires the conditions

$$\begin{aligned} A_{K^0nn} &= A_{K^0pp} + A_{K^+pn}, \\ B_{K^0nn} &= B_{K^0pp} + B_{K^+pn}, \end{aligned} \tag{16}$$

which are easily seen to be satisfied.

The third meson considered here is the σ meson, which is a scalar and isoscalar meson with the couplings

$$\begin{aligned} \mathcal{H}_s^{\sigma NN} &= g_s \bar{\psi}_N(x)\phi_\sigma(x)\psi_N(x), \\ \mathcal{H}_w^{\sigma\Lambda N} &= g_w \bar{\psi}_n(x)(A_\sigma + B_\sigma\gamma_5)\phi_\sigma(x)\psi_\Lambda(x). \end{aligned} \tag{17}$$

The weak Hamiltonian $\mathcal{H}_w$ consists of a parity-conserving part (proportional to A_σ) and a parity-violating part (B_σ). We employ 550 MeV for the mass of σ and 1200 MeV for the cutoff mass. From the medium-range attraction in the nuclear force potential, the strong coupling constant is known to be about 10, but here it is taken to be the same as the strong πNN coupling strength, i.e., $g_{\sigma NN} = g_{\pi NN}$. The results do not depend on the choice of $g_{\sigma NN}$, because it is always multiplied by the weak coupling constants A_σ or B_σ, which are free parameters in the present analysis. As mentioned already, the $\sigma\Lambda N$ coupling contains only the $\Delta I = 1/2$ transition because the σ meson is isoscalar. Unlike the OPE and OKE potentials, this potential does not include the tensor transition potential in a parity-conserving channel. Hence the OSE cannot affect the ${}^3S_1 \to {}^3D_1$ channel (d_p).

The DQ potential is given as the nonlocal form

$$\begin{aligned} V_{DQ}{}_{SS'J}^{LL'}(r,r') = -\frac{G_F}{\sqrt{2}} W \sum_{i=1}^{7} \big\{ & V_i^f f_i(r,r') \\ & + V_i^g g_i(r,r') + V_i^h h_i(r,r') \big\}, \end{aligned} \tag{18}$$

where r (r') stands for the radial part of the relative coordinate in the initial (final) state. The explicit forms of f_i, g_i, and h_i are given in Ref. [15], and the coefficients V_i^k for the $\Lambda N \to NN$ transitions are also listed in Ref. [15].

III. PHENOMENOLOGICAL ANALYSIS

Recently, Alberico and Garbarino [47] carried out an analysis of experimental data of the nonmesonic (NM) decays of the s-shell hypernuclei from the viewpoint of validity of the $\Delta I = \frac{1}{2}$ rule. Comparing analyses with and without the constraint from $\Delta I = \frac{1}{2}$, they found that the current experimental data can neither confirm nor deny its validity. Here we follow their analysis with new experimental data and study qualitative features of the decay rates in specific flavor and spin channels.

The data employed in the analyses are summarized in Table III, where we use the new data of the total NM decay rate and $\gamma \equiv \Gamma_n/\Gamma_p$ ratio of ${}^5_\Lambda$He taken from Ref. [26] and compare the results with those obtained from the old data in Ref. [19]. Among these data, the nonmesonic decay rate of ${}^4_\Lambda$H is the most ambiguous one. We take the weighted average of a recent estimate by Outa [21] and an old estimate by Block and Dalitz [37], but it should be noted that these numbers were not obtained by direct measurements but were estimated with theoretical assumptions.

We assume that the nonmesonic decay rates of the s-shell hypernuclei are parametrized as

$$\begin{aligned} \Gamma_{NM}\left({}^4_\Lambda\mathrm{H}\right) &= \Gamma_p\left({}^4_\Lambda\mathrm{H}\right) + \Gamma_n\left({}^4_\Lambda\mathrm{H}\right), \\ \Gamma_p\left({}^4_\Lambda\mathrm{H}\right) &= \frac{\bar{\rho}_4}{6} 2R_{p0}, \\ \Gamma_n\left({}^4_\Lambda\mathrm{H}\right) &= \frac{\bar{\rho}_4}{6}(R_{n0} + 3R_{n1}), \end{aligned} \tag{19}$$

TABLE III. Experimental data employed in the analysis in Sec. III, in units of $\Gamma_\Lambda^{\mathrm{free}}$. Set I includes the data employed in an analysis by Ref. [47]; set II comprises those for the present analysis.

	Set I	Set II
$\Gamma_{NM}({}^4_\Lambda\mathrm{H})$	0.22 ± 0.09 [47]	0.22 ± 0.09 [47]
$\Gamma_{NM}({}^4_\Lambda\mathrm{He})$	0.20 ± 0.03 [22]	0.20 ± 0.03 [22]
$\gamma_4^{\mathrm{He}} = \frac{\Gamma_n}{\Gamma_p}({}^4_\Lambda\mathrm{He})$	0.25 ± 0.13 [22]	0.25 ± 0.13 [22]
$\Gamma_{NM}({}^5_\Lambda\mathrm{He})$	0.41 ± 0.14 [19]	0.395 ± 0.016 [26]
$\gamma_5 = \frac{\Gamma_n}{\Gamma_p}({}^5_\Lambda\mathrm{He})$	0.93 ± 0.55 [19]	0.44 ± 0.11 [26]

TABLE IV. The results of analyses based on Eqs. (19)–(21) with and without the $\Delta I = 1/2$ constraint. Γ_{NM} are given in units of $\Gamma_\Lambda^{\rm free}$, and R_{NJ} are in units of fm^3.

	With $\Delta I = \frac{1}{2}$ rule		Without $\Delta I = \frac{1}{2}$ rule	
	Set I	Set II	Set I	Set II
R_{n0}	4.7 ± 2.1	6.1 ± 2.7	4.7 ± 2.1	6.1 ± 2.7
R_{p0}	2.3 ± 1.0	3.0 ± 1.3	$7.9^{+16.6}_{-7.9}$	22.8 ± 14.5
R_{n1}	10.3 ± 8.6	5.1 ± 3.0	10.3 ± 8.6	5.1 ± 3.0
R_{p1}	11.5 ± 6.7	15.2 ± 3.1	9.8 ± 5.5	8.7 ± 4.8
$\kappa = R_{n0}/R_{p0}$	2	2	$0.6^{+1.3}_{-0.6}$	0.27 ± 0.21
$\Gamma_{NM}({}^4_\Lambda\mathrm{H})$	0.17 ± 0.11	0.09 ± 0.03	0.22 ± 0.09 (input)	0.22 ± 0.09 (input)
$\gamma_4^{\rm H}$	7.6 ± 6.5	3.5 ± 2.2	$2.3^{+5.0}_{-2.3}$	0.47 ± 0.36

$$\begin{aligned}
\Gamma_{NM}\left({}^4_\Lambda\mathrm{He}\right) &= \Gamma_p\left({}^4_\Lambda\mathrm{He}\right) + \Gamma_n\left({}^4_\Lambda\mathrm{He}\right),\\
\Gamma_p\left({}^4_\Lambda\mathrm{He}\right) &= \frac{\bar\rho_4}{6}(R_{p0} + 3R_{p1}),\\
\Gamma_n\left({}^4_\Lambda\mathrm{He}\right) &= \frac{\bar\rho_4}{6}2R_{n0},
\end{aligned} \tag{20}$$

$$\begin{aligned}
\Gamma_{NM}\left({}^5_\Lambda\mathrm{He}\right) &= \Gamma_p\left({}^5_\Lambda\mathrm{He}\right) + \Gamma_n\left({}^5_\Lambda\mathrm{He}\right),\\
\Gamma_p\left({}^5_\Lambda\mathrm{He}\right) &= \frac{\bar\rho_5}{8}(R_{p0} + 3R_{p1}),\\
\Gamma_n\left({}^5_\Lambda\mathrm{He}\right) &= \frac{\bar\rho_5}{8}(R_{n0} + 3R_{n1}),
\end{aligned} \tag{21}$$

where R_{NJ} are the strengths of the $\Lambda N \to NN$ elementary interactions for the spin-singlet (R_{n0} , R_{p0}) and spin-triplet (R_{n1}, R_{p1}) channels. They are related to the $a \sim f$ amplitudes by

$$\begin{aligned}
\left|a_p^A\right|^2 + \left|b_p^A\right|^2 &= \frac{\bar\rho_A}{2(A-1)}R_{p0},\\
\left|a_n^A\right|^2 + \left|b_n^A\right|^2 &= \frac{\bar\rho_A}{2(A-1)}R_{n0},\\
\left|c_p^A\right|^2 + \left|d_p^A\right|^2 + \left|e_p^A\right|^2 + \left|f_p^A\right|^2 &= \frac{\bar\rho_A}{2(A-1)}R_{p1},\\
\left|f_n^A\right|^2 &= \frac{\bar\rho_A}{2(A-1)}R_{n1}.
\end{aligned} \tag{22}$$

The coefficient $\bar\rho_A$ denotes the average nucleon density at the position of Λ defined by

$$\bar\rho_A \equiv \int d\vec r\, \rho_A(\vec r)|\psi_\Lambda(\vec r)|^2. \tag{23}$$

There is an interesting theorem derived from the parametrization, Eq. (22). Define

$$R_4 \equiv \frac{\Gamma_{NM}\left({}^4_\Lambda\mathrm{H}\right)}{\Gamma_{NM}\left({}^4_\Lambda\mathrm{He}\right)},$$

and then it is straightforward to prove the following theorem, using the fact that all the R_{NJ} are positive.

Theorem:

$$\mathrm{Min}(\gamma_5, \kappa^{-1}) < R_4 < \mathrm{Max}(\gamma_5, \kappa^{-1}). \tag{24}$$

This theorem is extremely important because the ratio κ is directly related to ΔI in the weak transition. Namely, κ is determined solely by the Clebsch-Gordan coefficient when the isospin of the transition operator ΔI is purely 1/2 or 3/2, that is,

$$\kappa = \frac{\Gamma_n\left({}^4_\Lambda\mathrm{He}\right)}{\Gamma_p\left({}^4_\Lambda\mathrm{H}\right)} = \frac{R_{n0}}{R_{p0}} = \begin{cases} 2 & \text{for} \quad \Delta I = 1/2, \\ 1/2 & \text{for} \quad \Delta I = 3/2. \end{cases} \tag{25}$$

The new data [26] suggest $\gamma_5 \sim 0.5$. If we assume $\Delta I = 1/2$ or equivalently $1/\kappa = 1/2$, then the theorem restricts R_4 to be around 0.5. The current estimate of $\Gamma_{NM}({}^4_\Lambda\mathrm{H})$ does not seem to support $R_4 = 0.5$, although it is not completely rejected. In contrast, if we remove the $\Delta I = 1/2$ constraint, the theorem allows the two decay rates in $A = 4$ to be comparable, i.e., $R_4 \sim 1$, as the central values of the current estimate indicate.

Now we determine R_{NJ} from the two sets of the experimental data given in Table III. We first fix $\bar\rho_5$, again following Ref. [47] which uses an estimate from a model wave function such that $\bar\rho_5 = 0.045\ \mathrm{fm}^{-3}$. We also use this value throughout the phenomenological analysis in this section. In fact, the results are not sensitive to the choice of this value. This leaves five unknown parameters, $\bar\rho_4$ and four Γ_{NJ}, which can be determined by the five experimental data tabulated in Table III. In particular, the density parameter $\bar\rho_4$ can be determined by the relation

$$\frac{\Gamma_p\left({}^5_\Lambda\mathrm{He}\right)}{\Gamma_p\left({}^4_\Lambda\mathrm{He}\right)} = \frac{3\bar\rho_5}{4\bar\rho_4}, \tag{26}$$

where $\Gamma_p({}_\Lambda Z)$ is obtained by

$$\Gamma_p({}_\Lambda Z) = \Gamma_{NM}({}_\Lambda Z)[1 + \gamma({}_\Lambda Z)]^{-1}. \tag{27}$$

We obtain $\bar\rho_4 = 0.026\ \mathrm{fm}^{-3}$ for the data set I, while it is $0.020\ \mathrm{fm}^{-3}$ for set II.

The decay rates R_{NJ} determined by the two sets of data in Table III are given in the last two columns of Table IV. One sees that for both data sets the central value of κ is much smaller than 2, which indicates strong violation of the $\Delta I = \frac{1}{2}$ rule. The new data set significantly reduces the error bar and makes the conclusion prominent.

If we assume the $\Delta I = 1/2$ rule for the nonmesonic weak decays, then an extra condition $R_{n0}/R_{p0} = 2$ is imposed and it reduces the number of unknowns. Therefore, we can determine R_{NJ} without using $\Gamma_{NM}({}^4_\Lambda\mathrm{H})$ as an input. The first two columns of Table IV show the resulting R_{NJ}. The predicted value of $\Gamma_{NM}({}^4_\Lambda\mathrm{H})$ and the unknown n/p ratio of ${}^4_\Lambda\mathrm{H}$ are also given.

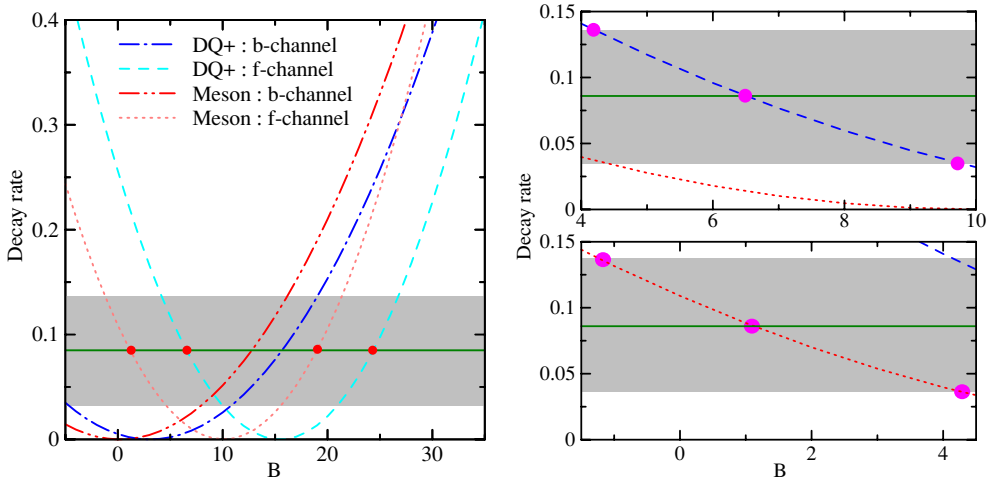

FIG. 1. (Color online) B_σ dependences of the partial decay rates in b_n and f_n channels given in units of Γ_Λ. The shaded region corresponds to R_{n1} evaluated in Sec. III. The right panels are the enlarged plots around the crossings for the f_n channel.

One sees that by imposing the $\Delta I = 1/2$ constraint, the ratio of R_{p0} and R_{p1} changes drastically, while the sum $(R_{p0} + 3R_{p1})$ remains constant. In fact, the order of R_{p0} and R_{p1} is reversed for set II. One also sees that $\Gamma_{NM}({}^4_\Lambda\mathrm{H})$ for set II is much smaller than the value given in Table II.

It is easy to prove the following two relations under the $\Delta I = 1/2$ constraint:

$$\frac{R_{n1}}{R_{n0}} = \frac{1}{3}\left(\gamma_4^{\mathrm{H}} - 1\right), \qquad \frac{R_{p1}}{R_{p0}} = \frac{1}{3}\left(\frac{4}{\gamma_4^{\mathrm{He}}} - 1\right). \tag{28}$$

The first equation gives a new constraint that γ_4^{H} must be larger than 1 if the $\Delta I = 1/2$ rule is satisfied. The second equation indicates that R_{p1} must be larger than R_{p0} because the n/p ratio of ${}^4_\Lambda$He is smaller than 1. These conditions may be useful for testing whether the $\Delta I = 1/2$ rule is satisfied. One can easily confirm that these relations are satisfied for our solutions with the $\Delta I = 1/2$ condition.

The conclusion of the phenomenological analyses of the decay rates and n/p ratios of the s-shell hypernuclei is that current experimental knowledge already suggests that the $\Delta I = 1/2$ rule is not satisfied in the NMWD, although precise measurements of the ${}^4_\Lambda$H decays are critical to finalizing the conclusion.

IV. ROLES OF THE σ-MESON EXCHANGE

The phenomenological analyses in the last section revealed that the new data for ${}^5_\Lambda$He reduce ambiguities in determining the partial decay rates, particularly for R_{n1}. In this section, we introduce a new element, i.e., the one-sigma exchange (OSE), in the microscopic model for the $\Lambda N \to NN$. A possible importance of OSE has been suggested by approaches in effective field theory for weak baryonic interaction. There a short-range weak transition with no charge or spin dependence seems to play a significant role in reproducing the decay rates and the proton asymmetry of NMWD.

We propose new microscopic models that incorporate OSE: (1) the meson exchange (ME) model, which contains OPE+OKE+OSE, and (2) the extended direct quark (DQ+) model, which consists of DQ+OPE+OKE+OSE. ME preserves the $\Delta I = 1/2$ rule, while DQ+ predicts significant violation of the $\Delta I = 1/2$ rule. The latter is induced by the effective four-quark Hamiltonian [8] and is a distinct feature of the direct quark interaction. We will see that both ME and DQ+ can reproduce the current experimental data more or less, but they predict differences in NMWDs of the $A = 4$ hypernuclei ${}^4_\Lambda$He and ${}^4_\Lambda$H.

Key quantities that show the importance of OSE are the partial decay rates f_N and b_N. In particular, $|f_n|^2$ is the only component of the R_{n1} decay rate and therefore can be determined from the experimental data rather directly.

Here we determine the weak $\Lambda n\sigma$ vertex parameters A_σ and B_σ. They are fixed in the following two steps. (1) We determine the parameter B_σ so as to reproduce the f_n and b_n decay rates. (2) Then A_σ is determined so that the total decay rate of ${}^5_\Lambda$He agrees with the recent experimental data [26].

Figure 1 shows the B_σ dependences of the b_n and f_n decay rates for both the ME and DQ+ cases. The $\Gamma(f_n)$, which is the decay rate of the f_n channel, is quadratic in B_σ, so that we have two candidates of B_σ. This is the channel that has contributions from OPE, OKE, and DQ all added up coherently and thus plays the central role in solving the n/p ratio problem. Our previous analysis employing the OPE+OKE+DQ model [15,18] was shown to give too much enhancement of $\Gamma(f_n)$ so that both the total decay rate and the n/p ratio of ${}^5_\Lambda$He were overestimated. The same enhancement is seen in Fig. 1 at $B_\sigma = 0$. Thus, the main role of the parity-violating part of OSE is that it reduces $\Gamma(f_n)$ so as to fit R_{n1}.

Between the two possibilities for B_σ, the larger one is not appropriate. This can be seen from the behavior of the other

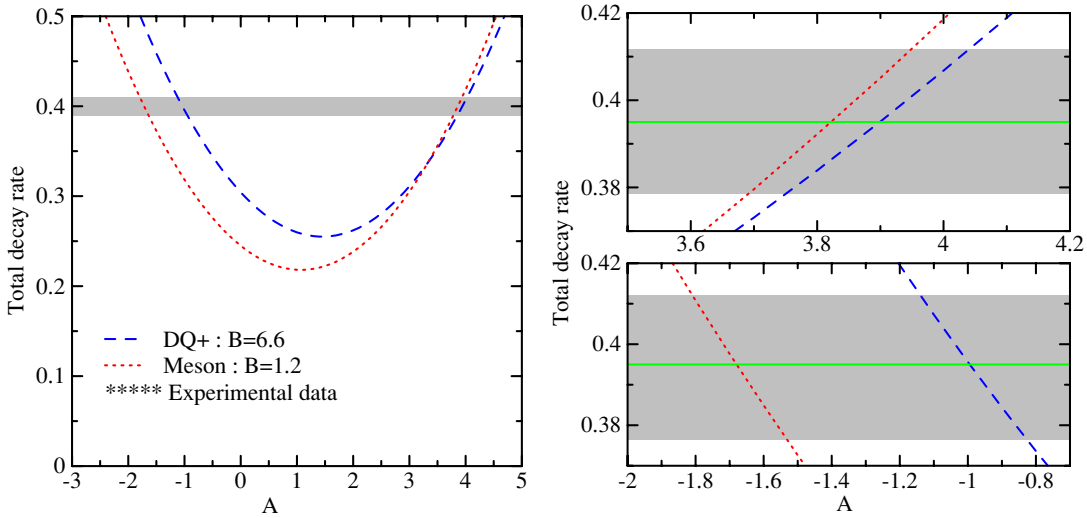

FIG. 2. (Color online) A_σ dependence of the total NM decay rate of ${}^{5}_{\Lambda}$He in the ME and DQ+ models given in units of Γ_Λ. The shaded region stands for the experimental value [26] with the error bar. Right two panels are enlargements of the intersections with the experimental values.

PV decay rate, $\Gamma(b_n)$, in Fig. 1. If we take the larger B_σ (i.e., $\sim$20), $\Gamma(b_n)$ becomes too large, $\sim 0.3\,\Gamma_\Lambda$, to accommodate the observed total decay rates. Thus we find the ranges for possible B_σ in the ME and DQ+ as

$$B_\sigma = \begin{cases} -1.2 \ \text{to} \ 4.4 \ \text{for ME}, \\ 4.2 \ \text{to} \ 9.8 \ \text{for DQ+}. \end{cases} \tag{29}$$

In fact, the central value of R_{n1} is reproduced by $B_\sigma = 1.2$ for ME and $B_\sigma = 6.6$ for DQ+.

Figure 2 shows the A_σ dependence of the total NM decay rate of ${}^{5}_{\Lambda}$He at the central value of B_σ. Because a_N and c_N depend linearly on A_σ, the total decay rate is a quadratic function of A_σ. Thus we again have two candidates of A_σ given by

$$A_\sigma = \begin{cases} 3.8 \ \text{and} \ -1.7 \ \text{for ME}, \\ 3.9 \ \text{and} \ -1.0 \ \text{for DQ+}. \end{cases} \tag{30}$$

Next, in Fig. 3 we show the A_σ dependences of the n/p ratio and the asymmetry parameter α of the NMWD of ${}^{5}_{\Lambda}$He. One sees in the left panel that the n/p ratio hits the peak at $A_\sigma = 1$ for ME, while the same value gives the minimum of the total NM decay rate of ${}^{5}_{\Lambda}$He. In contrast, for the DQ+ case, the maximum is given at $A_\sigma = -1$ and the minimum appears at $A_\sigma = 4$. For both ME and DQ+, positive A_σ around 4.0 gives a lower n/p ratio that is consistent with the experimental data.

The right panel of Fig. 3 shows the asymmetry parameter α. We find that it is sensitive to the choice of A_σ. For both ME and

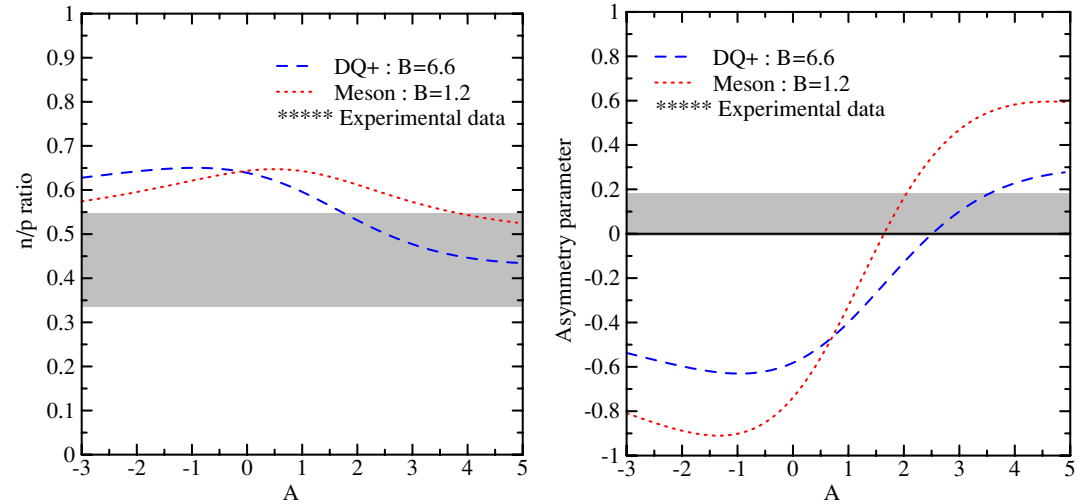

FIG. 3. (Color online) The A_σ dependences of the n/p ratio and the asymmetry parameter in ME and DQ+. The shaded region stands for the experimental values [26] with the error bar.

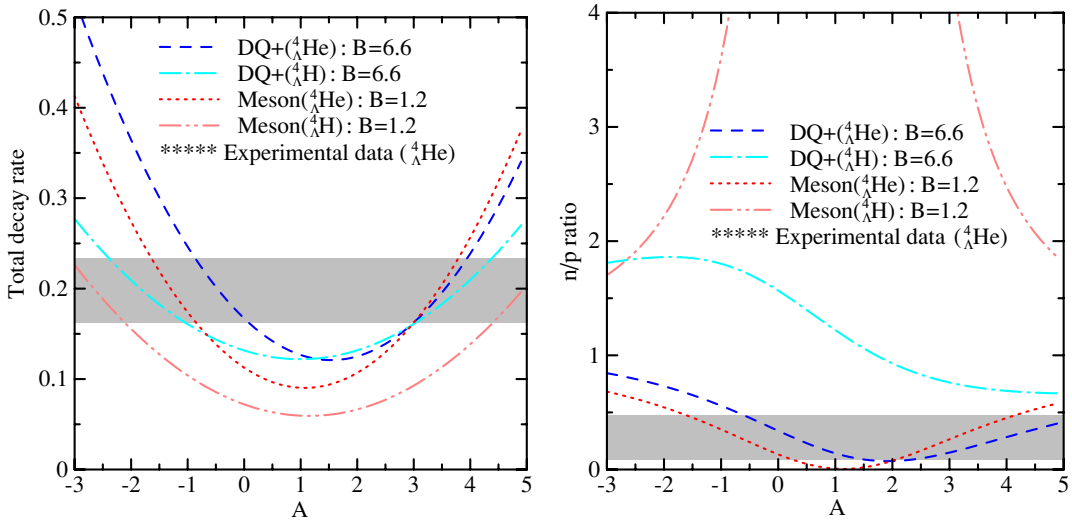

FIG. 4. (Color online) The total decay rates and n/p ratios of four-body hypernuclei are calculated by meson and DQ+ models in units of Γ_Λ. The shaded region stands for the experimental value of $^4_\Lambda$He [19] with error bar.

DQ+, α becomes large and negative around $A_\sigma = -1$, while it is positive around $A_\sigma = 4$. The value rises rather rapidly around $A_\sigma = 1$. The current experimental data for α are small but positive and therefore favor the positive A_σ.

The observables of $A = 4$ hypernuclei are also important to understand the $\Lambda N \to NN$ weak interactions, especially in the $J = 0$ transition channels. Figure 4 shows the A_σ dependences of the total NM decay rates and n/p ratios of both $^4_\Lambda$He and $^4_\Lambda$H. The experimental data of $^4_\Lambda$He are also shown in the figure. One sees that the total NM decay rate and the n/p ratio of $^4_\Lambda$He are reproduced within the experimental error bar at $A_\sigma = 4$ for both ME and DQ+.

The n/p ratio of $^4_\Lambda$H is interesting because it shows a clear difference between ME and DQ+. For ME, the n/p ratio has a huge peak at $A_\sigma = 1$, where the a-channel decay rate is extremely small. It is also seen that this ratio never falls lower than 1 which is consistent with the $\Delta I = 1/2$ condition given in the previous section. In contrast, the n/p ratio calculated by DQ+ model can be lower than 1, and it becomes 0.7 around $A_\sigma = 4$. Therefore, the n/p ratio of $^4_\Lambda$H is a key quantity to determine the property of the $\Lambda N \to NN$ weak interaction.

The results of the parameter searches in the ME model are summarized in Table V. We take three values for the parameter B_σ, corresponding to the upper, central, and lower values for R_{n1}, respectively. Then two solutions for A_σ are given for each B_σ because the total decay rate of $^5_\Lambda$He is a quadratic function of A_σ. Table V shows that the main difference between the positive and negative A_σ appears only in the asymmetry parameter, α, and its experimental value prefers the positive A_σ. We find that the γ_5, n/p ratio of $^5_\Lambda$He, prefers the smaller R_{n1} (the larger B_σ), while for the $\gamma_4^{\rm He}$ the larger R_{n1} (the smaller B_σ) is favorable.

The results for $A_\sigma = 3.8$ and $B_\sigma = 1.2$ give a reasonable account of most of the observables except the asymmetry parameter α. It is found that the total decay rate of $^4_\Lambda$H is about a half of $^4_\Lambda$He and the n/p ratio is about 2.7. One can easily check that these values satisfy the conditions for $\Delta I = 1/2$ given in the previous section.

Table VI shows the results for the DQ+ model. Again two solutions for A_σ can reproduce the total decay rate of $^5_\Lambda$He, but the positive A_σ explains all the available experimental data for both $A = 4$ and 5 hypernuclei fairly well. The negative A_σ tends to overestimate the n/p ratio of all hypernuclear systems, and therefore this choice is ruled out.

The calculation with $A_\sigma = 3.9$ and $B_\sigma = 6.6$ gives the best agreement with all the experimental data. In particular, we note

TABLE V. The nonmesonic decay rates, Γ_{NM}, the n/p ratios, γ, and the proton decay asymmetry parameter, α, predicted in the ME model. The decay rates are given in units of Γ_Λ.

	A_σ	3.0	−0.8	3.8	−1.7	4.5	−2.3	EXP
	B_σ	−1.2		1.2		4.4		
	Γ_{NM}	0.405	0.400	0.392	0.398	0.407	0.398	0.395 ± 0.016
$^5_\Lambda$He	γ_5	0.675	0.721	0.548	0.603	0.472	0.553	0.44 ± 0.11
	α	0.536	−0.857	0.571	−0.903	0.364	−0.684	0.07 ± 0.08
$^4_\Lambda$He	Γ_{NM}	0.199	0.195	0.235	0.240	0.298	0.291	0.20 ± 0.03
	$\gamma_4^{\rm He}$	0.219	0.249	0.417	0.492	0.692	0.781	0.25 ± 0.16
$^4_\Lambda$H	Γ_{NM}	0.132	0.135	0.128	0.138	0.145	0.151	0.22 ± 0.09
	$\gamma_4^{\rm H}$	6.400	5.946	2.705	2.488	1.379	1.362	—

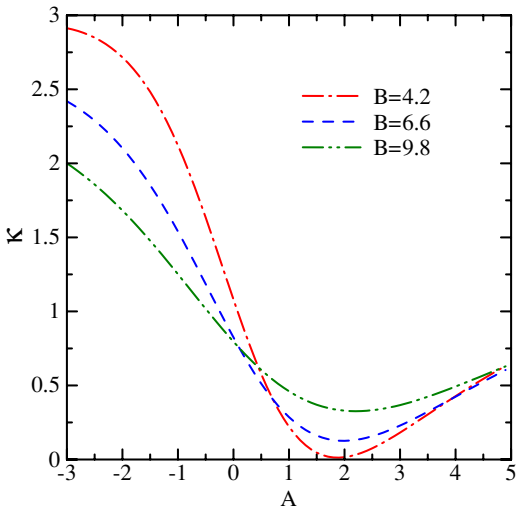

FIG. 5. (Color online) The A_σ and B_σ dependences of κ in the DQ+ model. If the $\Delta I = 1/2$ rule is preserved, the κ is equal to 2.

that the proton asymmetry parameter for ${}^{5}_{\Lambda}$He is predicted to be positive and small in this choice. It is brought mainly by OSE, which gives a major contribution to the $J = 0$ amplitudes. The σ exchange potential changes the sign of the a- and c-amplitudes from those without OSE and, thus, it leads to the drastic change of the proton asymmetry parameter, α.

The DQ+ model has a prominent feature that strongly violates the $\Delta I = 1/2$ rule. It is easily seen from the value of κ,

$$\kappa = \frac{\Gamma_n({}^{4}_{\Lambda}\mathrm{He})}{\Gamma_p({}^{4}_{\Lambda}\mathrm{H})} = 0.42. \tag{31}$$

Because $\Delta I = 1/2$ will lead to $\kappa = 2$, this result indicates a large violation of the $\Delta I = 1/2$ rule due to the DQ contribution. It is also seen from the total NM decay rates of ${}^{4}_{\Lambda}$He and ${}^{4}_{\Lambda}$H, which are almost equal, and the n/p ratios for $A = 4$, which are less than 1. As is shown in the previous section, these properties also indicate a large $\Delta I = 3/2$ contribution.

It is interesting to see the A_σ and B_σ dependencies of κ, illustrated in Fig 5. In the $B_\sigma = 4.2$ case that corresponds to the upper limit of R_{n1}, κ hardly changes with A_σ. All the curves cross the $\kappa = 2$ line in the region of negative A_σ. Therefore, it must be noted that there is the possibility of observing $\kappa = 2$ accidentally, even if the $\Delta I = 1/2$ rule is largely broken in the elementary vertex. Our choice, however, is $A_\sigma \sim 4$, where κ takes a value around 0.5. Thus our best-fit parameter set indicates the violation of the $\Delta I = 1/2$ rule.

In total, we conclude that the overall agreement of the theoretical predictions with experimental data in the DQ+ model is much better than in the ME model. This suggests strongly that the violation of the $\Delta I = 1/2$ rule is also favored by the current data set, although the definite conclusion will be given only after a future precise measurement is made of the NM decay of ${}^{4}_{\Lambda}$H.

V. CONCLUSIONS

A microscopic picture of the $\Lambda N \to NN$ weak interaction has been established including exchange of a scalar-isoscalar meson σ, i.e., one-scalar-exchange interaction. Our full model, called the DQ+ model, consists of the short-range DQ interaction as well as the long-range $\pi + K + \sigma$ exchange interactions. We have found that the new data for ${}^{5}_{\Lambda}$He are very powerful in determining the weak $\sigma N \Lambda$ coupling constants. They reduce ambiguity of the R_{n1} decay rate, which in turn determines the PV $\sigma N \Lambda$ coupling B_σ rather precisely. The PC part A_σ can then be determined by the total NM decay rate of ${}^{5}_{\Lambda}$He.

The established DQ+ model has been shown to reproduce fairly well all the current experimental data of four- and five-body hypernuclei. In particular, the asymmetry parameter of the proton emitted from polarized ${}^{5}_{\Lambda}$He is now consistent with recent experimental data.

A parallel analysis by the meson exchange (ME) model without the DQ part of the interaction is also found to explain most of the experimental data except for the asymmetry parameter, although the fit seems better in DQ+. The main difference between ME and DQ+ is in the isospin property. The ME interactions preserve the $\Delta I = 1/2$ rule and predict a small decay rate and a large n/p ratio in the NM decay of ${}^{4}_{\Lambda}$H. The DQ+ model, on the other hand, shows a larger decay rate, comparable to that of the NM decay of ${}^{4}_{\Lambda}$He, and a smaller n/p ratio in the ${}^{4}_{\Lambda}$H decay. Our analysis shows that the DQ+ model introduces a significant $\Delta I = 3/2$ contribution brought by the effective four-quark Hamiltonian and thus

TABLE VI. The nonmesonic decay rates, Γ_{NM}, the n/p ratios, γ, and the proton decay asymmetry parameter, α, predicted in the DQ+ model. The decay rates are given in units of Γ_Λ.

	A_σ	3.1	−0.2	3.9	−1.0	4.4	−1.5	EXP
	B_σ	4.2		6.6		9.8		
	Γ_{NM}	0.397	0.398	0.395	0.396	0.401	0.401	0.395 ± 0.016
${}^{5}_{\Lambda}$He	γ_5	0.593	0.750	0.449	0.650	0.367	0.585	0.44 ± 0.11
	α	0.248	−0.640	0.219	−0.630	−0.005	−0.400	0.07 ± 0.08
${}^{4}_{\Lambda}$He	Γ_{NM}	0.184	0.196	0.229	0.246	0.288	0.308	0.20 ± 0.03
	γ_4^{He}	0.091	0.274	0.269	0.559	0.498	0.870	0.25 ± 0.16
${}^{4}_{\Lambda}$H	Γ_{NM}	0.179	0.150	0.204	0.161	0.244	0.192	0.22 ± 0.09
	γ_4^{H}	1.396	3.649	0.693	1.802	0.411	0.979	—

predicts violation of the $\Delta I = 1/2$ rule. Crude estimates from the present knowledge on the ${}^{4}_{\Lambda}$H decay show a large NM decay rate and thus support the violation of the $\Delta I = 1/2$ rule.

We again stress that a direct measurement of the ${}^{4}_{\Lambda}$H decay is indispensable to establishing the violation of the $\Delta I = 1/2$ rule and hope that such an experiment is realized in the near future.

ACKNOWLEDGMENTS

One of the authors, K.S., acknowledges a JSPS Research Fellowship for financial support. This work is supported in part by the Grant for Scientific Research (B)No.15340072 and (C)No.16540236 from the Ministry of Education, Culture, Sports, Science and Technology, Japan.

[1] C. Y. Cheung, D. P. Heddle, and L. S. Kisslinger, Phys. Rev. C **27**, 335 (1983).
[2] B. H. J. McKellar and B. F. Gibson, Phys. Rev. C **30**, 322 (1984).
[3] K. Takeuchi, H. Takaki, and H. Bandō, Prog. Theor. Phys. **73**, 841 (1985).
[4] E. Oset and L. L. Salcedo, Nucl. Phys. **A443**, 704 (1985).
[5] J. F. Dubach, Nucl. Phys. **A450**, 71c (1986).
[6] H. Bando, Y. Shono, and H. Takaki, Int. J. Mod. Phys. A **3**, 1581 (1988).
[7] M. Shmatikov, Phys. Lett. **B322**, 311 (1994); Nucl. Phys. **A580**, 538 (1994).
[8] T. Inoue, S. Takeuchi, and M. Oka, Nucl. Phys. **A577**, 281c (1994); Nucl. Phys. **A597**, 563 (1996).
[9] K. Maltman and M. Shmatikov, Phys. Lett. **B331**, 1 (1994).
[10] A. Ramos, E. Oset, and L. L. Salcedo, Phys. Rev. C **50**, 2314 (1994).
[11] K. Itonaga, T. Ueda, and T. Motoba, Nucl. Phys. **A585**, 331c (1995); **A639**, 329c (1998); Phys. Rev. C **65**, 034617 (2002); Mod. Phys. Lett. A **18**, 135 (2003).
[12] J. F. Dubach, G. B. Feldman, B. R. Holstein, and L. de la Torre, Ann. Phys. **249**, 146 (1996).
[13] A. Parreño, A. Ramos, and C. Bennhold, Phys. Rev. C **56**, 339 (1997); A. Parreño and A. Ramos, *ibid.* **65**, 015204 (2002).
[14] T. Inoue, M. Oka, T. Motoba, and K. Itonaga, Nucl. Phys. **A633**, 312 (1998).
[15] K. Sasaki, T. Inoue, and M. Oka, Nucl. Phys. **A669**, 331 (2000); **A678**, 455(E) (2000).
[16] W. M. Alberico, A. De Pace, G. Garbarino, and R. Cenni, Nucl. Phys. **A668**, 113 (2000).
[17] D. Jido, E. Oset, and J. E. Palomar, Nucl. Phys. **A694**, 525 (2001).
[18] K. Sasaki, T. Inoue, and M. Oka, Nucl. Phys. **A707**, 477 (2002).
[19] J. J. Szymanski *et al*., Phys. Rev. C **43**, 849 (1991).
[20] H. Noumi *et al*., in *Proceedings of the IV International Symposium on Weak and Electromagnetic Interactions in Nuclei*, edited by H. Ejiri, T. Kishimoto, and T. Sato (World Scientific, Singapore, 1995), p. 550.
[21] H. Outa *et al*., Nucl. Phys. **A639**, 251c (1998).
[22] V. J. Zeps (E788 Collaboration), Nucl. Phys. **A639**, 261c (1998).
[23] H. Bhang *et al*., Phys. Rev. Lett. **81**, 4321 (1998); H. Park *et al*., Phys. Rev. C **61**, 054004 (2000).
[24] S. Ajimura *et al*., Phys. Rev. Lett. **84**, 4052 (2000).
[25] O. Hashimoto *et al*., Phys. Rev. Lett. **88**, 042503 (2002).
[26] H. Outa, in Proceedings of the VIII International Conference on Hypernuclear and Strange Particle Physics (HYP2003), Jefferson Lab, Newport News, Virginia, October 2003 (unpublished).
[27] K. Itonaga, T. Motoba, and T. Ueda, in *Proceedings of the Electrophoto Production of Strangeness on Nucleons and Nuclei*, edited by K. Maeda, H. Tamura, S.-N. Nakamura, and O. Hashimoto (World Scientific, Singapore, 2004), pp. 397–402.
[28] J.-H. Jun, Phys. Rev. C **63**, 044012 (2001).
[29] A. Parreño, C. Bennhold, and B. Holstein, nucl-th/0308074; A. Parreño, C. Bennhold, and B. Holstein, in Proceedings of the VIII International Conference on Hypernuclear and Strange Particle Physics (HYP2003), Jefferson Lab, Newport News, Virginia, October 2003 (unpublished); nucl-th/0312047.
[30] S. Eidelman *et al*. (Particle Data Group), Phys. Lett. **B592**, 1 (2004).
[31] M. Takizawa, T. Inoue, and M. Oka, Prog. Theor. Phys. (Suppl.) **120**, 335 (1995).
[32] K. Miura and T. Minamikawa, Prog. Theor. Phys. **38**, 954 (1967).
[33] J. C. Pati and C. H. Woo, Phys. Rev. D **3**, 2920 (1971).
[34] E. A. Paschos, T. Schneider, and Y. L. Wu, Nucl. Phys. **B332**, 285 (1990).
[35] G. Altarelli and L. Maiani, Phys. Lett. **B52**, 351 (1974).
[36] A. I. Vainshtein, V. I. Zakharov, and M. A. Shifman, Sov. Phys. JETP **45**, 670 (1977).
[37] M. M. Block and R. H. Dalitz, Phys. Rev. Lett. **11**, 96 (1963).
[38] C. B. Dover, Few-Body Systems (Suppl.) **2**, 77 (1987).
[39] R. A. Schumacher, Nucl. Phys. **A547**, 143c (1992).
[40] H. Nabetani, T. Ogaito, T. Sato, and T. Kishimoto, Phys. Rev. C **60**, 017001 (1999).
[41] B. F. Gibson, A. Goldberg, and M. S. Weiss, Phys. Rev. C **6**, 741 (1972).
[42] Y. Akaishi, T. Harada, S. Shinmura, and Khin Swe Myint, Phys. Rev. Lett. **84**, 3539 (2000).
[43] E. Hiyama, M. Kamimura, T. Motoba, T. Yamada, and Y. Yamamoto, Phys. Rev. C **65**, 011301 (2002).
[44] A. Nogga, H. Kamada, and W. Glöckle, Phys. Rev. Lett. **88**, 172501 (2002).
[45] H. Nemura, Y. Akaishi, Y. Suzuki, Phys. Rev. Lett. **89**, 142504 (2002).
[46] Th. A. Rijken, V. G. J. Stoks, and Y. Yamamoto, Phys. Rev. C **59**, 21 (1999); V. G. J. Stoks and Th. A. Rijken, *ibid.* **59**, 3009 (1999).
[47] W. M. Alberico and G. Garbarino, Phys. Lett. **B486**, 362 (2000); Phys. Rep. **369**, 1 (2002).